



Transmission-enhancing effects of a plant virus depend on host association with beneficial bacteria

Milica Nenadić^{1,2} · Luca Grandi^{1,3} · Mark C. Mescher¹ · Consuelo M. De Moraes¹ · Kerry E. Mauck^{1,4}

Received: 16 September 2021 / Accepted: 6 December 2021
© The Author(s), under exclusive licence to Springer Nature B.V. 2021

Abstract

Vector-borne viruses can alter host-plant chemistry and thereby influence interactions between plants and vectors, frequently in ways that enhance their own transmission. However, these interactions may also be influenced by the presence of other symbiotic microorganisms, including co-evolved plant mutualists. Here, we explore how rhizobia colonization influences plant virus effects on host chemistry, vector behavior, and virus transmission using a system consisting of *Medicago truncatula*, *Alfalfa mosaic virus* (AMV), its aphid vector *Acyrtosiphon pisum*, and the rhizobial symbiont *Sinorhizobium*. We hypothesized that virus effects and outcomes for virus transmission would differ when plants were co-colonized by rhizobia, which are known to alter both defense gene expression and nutritional status of their hosts. Consistent with this hypothesis, we found that aphid dispersal following virus acquisition was greatest from AMV-infected plants with rhizobia, and that this translated into increased rates of transmission in mesocosm experiments. These effects are likely mediated by rhizobial and viral effects on plant defense responses and primary metabolites. AMV infection also suppressed volatiles across both rhizobia treatments, which contrasts with previous reports of viruses enhancing host volatiles. However, aphids did not exhibit odor-based preferences, suggesting volatiles may not be important mediators of host choice or targets for manipulation by AMV. Collectively, this study provides evidence that putative virus manipulations of hosts and vectors depend on the pre-existing physiological condition of the host—in this case, presence of a co-evolved intracellular root symbiont.

Keywords Aphids · Plant volatiles · Phytohormones · Virus manipulation

Handling Editor: Heikki Hokkanen

✉ Kerry E. Mauck
kerry.mauck@ucr.edu

Milica Nenadić
milica.nenadic@botinst.uzh.ch

Luca Grandi
lgrandi@invaio.com

Mark C. Mescher
mescher@usys.ethz.ch

Consuelo M. De Moraes
consuelo.demoraes@usys.ethz.ch

¹ Department of Environmental Systems Science, ETH Zürich, 8092 Zürich, Switzerland

² Department of Plant and Microbial Biology & Zurich-Basel Plant Science Centre, University of Zurich, 8008 Zurich, Switzerland

³ Invaio Sciences International GmbH, 4051 Basel, Switzerland

⁴ Department of Entomology, University of California, Riverside, Riverside, CA 92521, USA

Introduction

Vector-borne pathogens of plants and animals often alter traits of their hosts in ways that influence subsequent interactions with insect vectors, with implications for pathogen transmission and epidemiology (Lefèvre and Thomas 2008; Roosien et al. 2013; Shaw et al. 2017, 2019). Effects on plant chemistry play a central role in mediating such interactions; yet, the chemical ecology of pathogen-host-vector interactions has been examined in relatively few pathosystems, mainly involving viral pathogens. A growing number of studies have explored virus effects on chemically mediated interactions between plants and vector and non-vector insects (reviewed in Mauck et al. 2018). The patterns of effects revealed by these studies suggest that virus transmission mechanisms may play an important role in shaping the evolution of pathogen effects on biochemically mediated plant traits, including nutrition, defense chemistry, and plant-derived olfactory cues. For example, viruses that can only be acquired by vectors during prolonged feeding on

infected vascular tissues tend to improve plant palatability and quality, while those that can be acquired during short probes of non-vascular tissue tend to reduce host quality and thereby promote rapid vector dispersal (Mauck et al. 2012, 2016, 2018). The convergence of such patterns across divergent virus taxa strongly suggests adaptive evolution of virus effects on host-plant chemistry. However, because most studies to date have focused on highly simplified pathosystems, we currently have little information about how virus-plant-vector interactions play out in more natural settings, where viral pathogens frequently co-occur with other plant symbionts, including some that may have conflicting interests with respect to effects on plant chemistry.

Another limitation of the existing literature is that a large majority of studies to date have focused on domesticated crops (Mauck et al. 2018; Mauck and Chesnais 2020). For example, in a recent review, we found that wild plants only constituted 12% of all published experiments exploring aspects of plant virus manipulation of hosts and vectors (Mauck et al. 2018). While this focus is understandable given the historical focus of plant virology on agriculturally relevant interactions, it neglects the prevalence and likely ecological significance of virus infection in wild plant populations. For example, nearly all virome studies to date have reported that a large majority of wild plants host one or more virus infections (Shates et al. 2018; Maclot et al. 2020). Furthermore, virus infection of wild species can also have relevance for agriculture, as wild plant populations frequently serve as reservoirs for viruses that circulate into and out of seasonally abundant crop hosts (McLeish et al. 2019). Despite this clear evidence that viruses are both abundant and important in non-crop hosts, only a handful of studies on virus manipulation have focused on interactions in wild pathosystems.

The present study aims to address these shortcomings of our current understanding of virus manipulation through investigation of a wild virus-host-vector system comprising a leguminous non-crop host plant (*Medicago truncatula*), a Fabaceae-adapted virus (*Alfalfa mosaic virus* [AMV], genus *Alfamovirus*, family *Bromoviridae*), and a legume-specialist aphid (*Acyrtosiphon pisum*). In addition, we explore how virus effects on plant chemistry and vector behavior are influenced by the presence of a mutualistic plant symbiont (*Sinorhizobium meliloti*), a nitrogen-fixing bacteria that stimulates the formation of protective root nodules in *Medicago* spp. We hypothesized that AMV effects on plant phenotype and vector behavior, and their outcomes for virus transmission, will differ depending on whether the host plant is in symbiosis with *S. meliloti*. Given the ubiquity of this symbiosis, it is possible that AMV infections (and host manipulations) would most often take place in the presence of *S. meliloti* and any phenotypic alterations it has already induced. If

the host environment in which selection for manipulative traits occurs is therefore the microbe-altered host, and not the microbe-free host that is often used in the laboratory (Partida-Martínez and Heil 2011), we might expect that the virus would be more successful in manipulating the host and vector in the presence of *S. meliloti*. On the other hand, given that virus infections can be detrimental for host growth and survival, *S. meliloti* colonization might strengthen the plant's ability to resist infection, and thereby, manipulation.

Our hypothesis is based on a growing body of research showing that root-associated microbes strongly influence plant growth, immunity, physiology, and chemistry in ways that alter plant interactions with other organisms (Friman et al. 2020; Olowe et al. 2020; Cachapa et al. 2021; Löser et al. 2021). During the process of establishing intracellular symbioses, rhizobia engage in a dialogue with the host plant that involves suppression of anti-pathogen defenses via ligands acting intracellularly (e.g. nodulation outer proteins) and extracellularly (e.g. Nod factors) (Gourion et al. 2015). Once established in intracellular symbiosis, rhizobia continue to express and secrete effectors that regulate perception of, and responses to, microbe-associated molecular patterns at the transcriptional level (Gourion et al. 2015). Additionally, by provisioning of nitrogen, rhizobia in established nodules can augment the nutritional composition of the host and availability of nitrogen for synthesis of costly secondary metabolites and other defenses.

Rhizobial effects on plant nutritional and defense phenotypes can subsequently influence responsiveness to other pathogens (including viruses) as well as defenses against herbivores via crosstalk between core pathogen and insect defense pathways. For example, in lima bean, association with rhizobia improved plant growth and both direct (leaf cyanogenic compounds) and indirect (odor-mediated) defense against a specialist chewing herbivore (Thamer et al. 2011; Ballhorn et al. 2013). And in soybean, rhizobial associations modify defense induction and interactions with both chewing and piercing-sucking herbivore pests (Dean et al. 2009, 2014). Rhizobial effects on plant virus infections are relatively less well-studied compared to rhizobial effects on plant-insect interactions, but there is evidence that *Sinorhizobium* bacteria can reduce virus susceptibility in *Medicago* and other hosts (Wahyuni and Randles 1993). More recently, we found that *Bradyrhizobium* symbiosis in combination with a second, non-nitrogen fixing rhizobacteria (*Delftia acidovorans*) counteracted suppression of indirect defenses caused by *Bean pod mottle virus* (BPMV) infection in soybean (Pulido et al. 2019). In this system, BPMV-infected plants with both root microbes were able to recruit parasitoids of the beetle herbivore that transmits the virus to the same extent as virus-free hosts, while BPMV infection in the absence of the microbes strongly suppressed

vector-induced volatile emissions and parasitoid attraction (Pulido et al. 2019).

The work proposed here builds upon our prior study involving soybean, BPMV, and *Bradyrhizobium* by examining the effects of a different co-evolved rhizobial symbiont, *Sinorhizobium*, on virus fitness, biochemically mediated plant traits, and patterns of interaction among host plants and aphid vectors using a well-characterized model legume, *Medicago truncatula*. Infection of *Medicago* species by plant viruses is frequent and well-documented. The suite of viruses most found in *Medicago* includes several pathogens transmitted by aphids in a non-persistent manner, meaning that the acquisition and inoculation of virions occurs during short probes instead of long-term feeding bouts. Thus, virus transmission is enhanced when aphids are attracted to infected plants, but then encouraged to disperse following acquisition of taste cues and virions (Martin et al. 1997; Wang and Ghabrial 2002). In mixed pastures of *Medicago*, virus infection typically spreads outward from focal infections via the probing and dispersal of non-winged, *Medicago*-colonizing vector aphids (Jones 2012)—a pattern suggesting that some of the viruses frequently infecting *Medicago* may induce changes in the host plant that encourage aphid visitation, virion acquisition, and subsequent dispersal. Here, we worked with one of these non-persistently transmitted pathogens—*Alfalfa mosaic virus* (AMV, genus *Alfamovirus*, family *Bromoviridae*) which is prevalent in fields dominated by *M. truncatula* (Dall et al. 1989; Barbetti et al. 2020) and is transmitted by at least 14 aphid species, including the species used in the present study (*Acyrtosiphon pisum*).

Materials and methods

Plant, bacteria, virus, and insect culture

Seeds of *Medicago truncatula* of genotype “Jemalong A17” were propagated from seed stock provided by the United States Department of Agriculture National Plant Germplasm System. Seeds were stored in pods to ensure longevity. To germinate seeds, we crushed seed pods gently with pliers to release seeds, then scarified each seed coat surface with ultra-fine sandpaper. We sterilized seeds by soaking in a 2.6% sodium hypochlorite solution for two minutes followed by five rinses with Milli-Q sterile water. We germinated seeds by positioning on plates of 0.8% water agar and incubating for three days in the dark at 24 °C. We transplanted seedlings into pots (dimensions: 10, 8, 8 cm) containing a 1:1 mixture of sand: perlite, which had been washed and sterilized by autoclaving at 121 °C for 30 min. Seedlings were fertilized with 5 ml of nitrogen-rich nutrient solution (Dean et al, 2014) and watered with Milli-Q

water. We maintained plants in Conviron reach-in growth chambers with 16:8-h (light: dark) photoperiod at 22 °C, and relative humidity of 60%. Plants were fertilized with 5 mL of nitrogen-rich solution at three and five days after transplanting. At seven days post transplanting, half of the plants in a given set were inoculated with *Sinorhizobium* bacteria (see culture conditions below). Plants were used at 6–7 weeks post planting unless otherwise indicated.

Sinorhizobium spp. were isolated from nodules of *Medicago lupulina* collected in a field of mixed legumes adjacent to the ETH Hönggerberg campus, Switzerland, using protocols described in Somasegaran and Hoben (1994). In brief, nodules were surface sterilized first in 95% ethanol (to break surface tension) and then in 2.6% sodium hypochlorite, rinsed with sterile water, and placed in sterile, conical bottom eppendorf tubes containing sterile water and housed in a laminar flow hood. Using a sterile plastic pestle, we crushed nodules and streaked water contents onto yeast-mannitol agar (YMA) media using a sterile 1 mm loop. After 4 days, these primary isolation plates were examined for colonies with morphology consistent with *Sinorhizobium* spp. Single colonies were subsequently picked and streaked onto three types of plates for further strain-specific isolation: YMA + bromothymol blue, YMA + congo red, and peptone glucose agar. Following incubation for four days, the plates were examined for colony structure and color. The final isolate was selected from a set of plates produced from a single primary isolation colony, and yielding colony features indicative of *S. meliloti*: characteristic mucoid morphology on both YMA plates, uptake of congo red dye, and a positive reaction to the bromothymol blue test. We also looked for a lack of growth on peptone-glucose agar.

A single colony was selected from several potential isolates fitting *Sinorhizobium* colony morphology criteria and further cultured in YMA media by shaking at 24 °C for 3–4 days. Each culture was screened for compatibility and nitrogen-fixing capacity by inoculating to young seedlings of *M. truncatula* growing in sterile potting mix. The final isolate used in experiments was selected based on nodulation efficiency and similarity in growth and size among plants receiving inoculum for that isolate relative to control plants receiving 2 g of slow release Osmocote fertilizer. Nodules were collected from a single individual receiving the selected isolate, and the re-isolation process was repeated to ensure purity of the culture. Stocks were grown in YMA broth and mixed in a 50:50 ratio with sterile glycerol in cryovials, then stored at – 80 °C.

Plant inoculation followed protocols described by Gourion et al. (2015). We began cultures by streaking our *S. meliloti* isolate from preserved stocks onto YMA and peptone glucose agar plates five days before inoculation of plants used in experiments. All transfers were performed in a laminar flow hood using sterile technique. Bacteria were

left to grow for two days at 24 °C. After confirming colony morphology and lack of growth on peptone glucose agar plates, we created liquid cultures by inoculating a single colony in 2 ml TA liquid medium. Cultures were incubated for two days at 24 °C, then we transferred 1 mL of broth culture from each vial into a matching flask with 30 ml of TA (1 flask per vial), which was sealed with cotton and aluminum. All materials were sterilized by autoclaving prior to use and transfers were performed using sterile technique in a laminar flow hood. Flasks were incubated as above for two days. We then transferred the contents of each flask to two 15 mL sterile Falcon tubes, then centrifuged for 10 min at 4 °C (2700 rpm). We removed the supernatant, and the resulting pellet was gently resuspended in 5 ml of autoclaved Milli-Q water. Resuspended bacteria were combined into one flask, and OD600 was measured using a SpectraMax I3 spectrophotometer (Molecular Devices). We adjusted the OD600 to 0.1 using sterile Milli-Q water and applied 2.5 mL of inoculum per pot. The same volume of sterilized Milli-Q water was applied to control plants. Three days following inoculation we instituted a new fertilization regimen. For one week, plants inoculated with *S. meliloti* received 10 ml of nitrogen-limited solution on Monday, Wednesday, and Friday. Simultaneously, control plants received 10 ml of nitrogen-rich nutrient solution. From week two post inoculation, plants received 20 ml of either solution on the same weekdays. Nitrogen-rich solution was used to avoid reduced growth of control compared to rhizobia inoculated plants, while the application of nitrogen-low solution ensured that both plant groups received the same externally applied nitrogen source. Details of nitrogen watering solutions are in the Supplementary Materials. All plants used in experiments were harvested and inspected for presence of root nodules following completion of assays to verify bacterial treatments.

Alfalfa mosaic virus (AMV) is a globally distributed virus in the genus *Alfavirus*, family *Bromoviridae* (ICTV). AMV is a causal agent of disease in pasture legumes (genus *Medicago*) where systemic infections can result in up to a 50% reduction in above-grown biomass as well as reductions in seed production and root nodulation (Dall et al. 1989). The virus also causes symptomless infections in many herbaceous, dicotyledonous hosts, and the experimental host range (in the laboratory) includes 430 species across 51 families (Jaspars and Bos 1980). AMV is transmitted by at least 14 species of aphids in a non-persistent manner (through short probes of non-vascular tissue), with some strains transmissible to seeds (from parent to ovule, or via pollen).

The AMV used in the present study was originally isolated from a *Medicago sativa* plant growing in a field of mixed legumes adjacent to the ETH Höggerberg campus. The isolated virus was propagated in *M. truncatula* to create a uniform stock culture of tissue to be used in all

experiments. Tissue was stored as individual doses in coin envelopes at – 80 °C. We inoculated plants using mechanical inoculation procedures when plants reached the 3rd week of growth post-planting. Each dose of virus used for inoculating a set of plants consisted of four leaves—two upper and two lower, from symptomatic positive hosts. Leaves were ground in 30 mL of 0.1 M potassium phosphate buffer at pH 7. We mixed inoculum with a small quantity of 400 mesh carborundum (silicon carbide) and 0.05 M sodium sulfite as a virion stabilizing additive, then rubbed the solution onto the adaxial side of all leaves through gentle brushing motion. Healthy plants were mock inoculated with buffer and carborundum only. All plants used in experiments were confirmed positive using an AMV ELISA kit produced by Bioreba AG. ELISA was performed in a semi-quantitative manner (standardizing tissue to buffer ratio) where appropriate to assess infection severity along with other virus effects.

Acyrtosiphon pisum were collected locally by colleagues at Agroscope Reckenholz, Switzerland (approximately 3 km from the location where the virus and bacteria were isolated) and maintained on *Vicia faba* under a 16:8 photoperiod and 25 °C. We confirmed that aphids originating from this culture can survive and reproduce on *M. truncatula*, and transmit the isolate of AMV, prior to beginning experiments. For all work, we used 4th instar nymphs to limit the effects of insect age on behavior and performance. Insects were collected by tapping source plants gently over a clear plastic box, after which cohorts were removed to small glass petri dishes. To limit movement, we kept insects cool during the transfer by suspending the box over a tray of ice.

Volatile-based aphid preferences

We used a Y-tube olfactometer to determine if virus or rhizobia-induced changes in plant volatiles influence the behavior of the vector. We focused on comparing healthy and infected plants within each bacterial inoculation treatment (5 pairs per comparison at 6–7 weeks old). The two choice plants were enclosed in glass domes (0.75 L) two hours prior to the assay. Glass domes consisted of lower and upper portions joined tightly with a gasket and metal clamp. Upon closure, charcoal-filtered, moistened air (via bubbler) was introduced through a port in the lower half at the rate of 0.5 L per minute, which was lost at the same rate through the port at the top of the dome. Before the experiment, the glass Y-tube arms were connected to the upper ports of domes via Teflon tubes to receive the outgoing air. The ends of the Y-tube arms were wrapped in a transparent green cellophane to provide a uniform visual cue, and each was illuminated behind the cellophane with LED lights of equal strength as in (Blackmer and Cañas 2005; Pulido et al. 2019). To eliminate visual distractions, the Y-tube was placed in a grey cardboard box without a lid. Since preliminary experiments

showed that the aphids do not walk readily on the glass of the olfactometer, a Y-shaped wooden rod was positioned in the center of the olfactometer, and aphids were released at the starting point on this rod.

Air was pulled from the olfactometer at the rate of 1 L per minute to ensure that the airflow from one arm did not enter the other arm. Aphids were starved for at least 3 h before the experiment. With a small paint brush, one aphid at a time was introduced at the base of the Y-tube and behavior was monitored for a 10-min period. We considered that the aphid made a choice if it crossed the 2nd half of either arm and remained in this region for the duration of the test. The olfactometer was switched every 10 aphids to present treatments from different arms and 20 aphids were tested per plant pair. Trials were carried out between 11:30 am and 4:00 pm over the course of 7 days. Between plant pairs, we rinsed glassware with acetone and hexanes, Teflon hoses with hexanes, and wooden rods with 96% ethanol. Prior to beginning tests with experimental plant pairs, we confirmed that aphids can locate potential host plants (fava beans) based on volatile cues presented in the olfactometer and confirmed that the cardboard box set-up prevents aphids from exhibiting positional bias. Each dual choice test was analyzed using chi-squared tests (Minitab v.17).

Contact-based aphid preferences

We evaluated aphid settling preferences using release-and-track choice tests similar to those performed in Mauck et al. (2010) and Mauck et al. (2014). We created arenas with two plants presented at opposite corners of a brown square platform housed in a 28 cm × 28 cm mesh cage with a viewing window (Bioquip). Cages were set up in an entirely darkened room and each was illuminated evenly from above with an LED shop light. One plant was designated as the “release” plant, and the other designated as the “choice” plant. Under chilled conditions (a surface cooled from below by an ice tray), we prepared cohorts of 32 4th instar aphids by gently placing them on a filter paper disc in a glass petri dish. The aphids remained still on the paper as long as they were kept cool. Prior tests demonstrated that aphids recover from chilling within minutes of returning to room temperature, even when cooled for several hours. Aphids were maintained in this way for approximately 45 min, then filter paper discs with aphids were transferred gently onto the “release” plant within each cage. Positions of aphids (paper, release plant, or choice plant) were evaluated at a short-term time point (2 h) and one long-term time point (24 h). Our primary goal was to compare dispersal of aphids from each treatment to plants of the opposite virus *or* bacterial status. A full factorial design was not logistically feasible, so we focused on the following tests: 1. AMV/*Sinorhizobium* (release) vs. *Sinorhizobium* only (choice), to mimic the scenario of an

AMV infected plant occurring in an environment where all plants have *Sinorhizobium* colonization; 2. AMV/control (release) vs. control (choice), to mimic the scenario of an AMV-infected plant occurring in an environment where all plants lack *Sinorhizobium* colonization; and *Sinorhizobium* only (release) vs. control (choice) and control (release) vs. *Sinorhizobium* (choice), to evaluate the effect of bacteria on aphid preferences in the absence of infection. Five experimental setups with 32 aphids per setup were evaluated for each pair of treatments. We analyzed the proportion of aphids dispersed from release plants at 2 h (when all aphids had left the paper) and 24 h as a product of bacterial treatment (fixed) virus treatment (fixed), and their interaction, using a general linear model (Minitab v.17).

Transmission assay

To evaluate whether bacterial influence on virus-induced host phenotypes alters aphid behavior in ways that are relevant for transmission, we performed a separate set of contact-based preference tests with a post-test assessment of choice plant infection status. Four transmission arenas were prepared for each infected source plant treatment (AMV/*Sinorhizobium* and AMV/Control), which were prepared according to the methods described in the organism culture section. In each arena, which consisted of a 27 cm × 27 cm × 10 cm plastic tray filled with potting soil, the central location was occupied by a 7-week-old release plant, which was surrounded by ten 17-day old *M. truncatula* seedlings as choice plants and placed in a 28 cm × 28 cm × 28cm cage. Twenty-four fourth instar aphids were collected onto filter paper discs in glass petri dishes as described above and starved for two hours. We released aphids onto the central plant by placing the filter paper disc gently into the center of the plant. After 24 h, aphids were carefully removed from the release plant and choice plants using an aspirator (to prevent human-induced movement and virus transmission). We removed plants from the cages, removed the release plant from the center, and carefully inspected all choice plants for aphids. Choice plants were treated with an insecticidal soap solution (Coop Oecoplan Biocontrol Insecticide) and grown for another two weeks, after which they were tested for AMV infection using ELISA (Bioreba AG). We calculated the percentage of seedlings that became infected due to aphids dispersing from each release plant type as a measure of virus transmission.

Plant growth parameter measurements

To evaluate interactive effects of virus infection and *S. meliloti* colonization on plant growth parameters, as well as reciprocal effects of each microbe on the others fitness, we grew three sets of plants to 48 days post planting using a

full factorial design and the inoculation methods described above. Each set had between 4 and 8 plants of each bacteria x virus treatment. At 28 and 48 days, tissue was sampled, weighed and preserved at $-80\text{ }^{\circ}\text{C}$ for a semi-quantitative ELISA assay to estimate virus titer (performed using the manufacturer's protocol, AMV ELISA kit from Bioreba AG). At 48 days post planting, all plants were harvested. Fresh shoot biomass was weighed and recorded, while roots were processed to remove sand by gentle washing. Surface water was removed with gentle pressure using paper towels and roots were weighed. Following collection of these data, roots of plants inoculated with *S. meliloti* were stored in moist paper towels at $4\text{ }^{\circ}\text{C}$ for several days, over which time nodules were counted to assess the impact of virus infection on *S. meliloti* colonization. Roots of control plants were evaluated to ensure they were free of *S. meliloti* colonization.

Metabolite profiling: Volatiles

We collected volatiles from 7-week-old plants using a push–pull collection system. Above-ground tissues were enclosed in 3.5L glass domes with a stainless-steel base fitted around the lower stem, covering the sand substrate. Charcoal-filtered air was introduced into each dome at a rate of 1.5L per minute and pulled from domes through an adsorbent (Hayesep-Q, 40 mg) at a rate of 1.0L per minute. This ensured positive pressure was maintained in the dome, preventing sampling of contaminants from outside the headspace. Volatiles were collected for 9 h from between 4 and 8 individuals of each bacteria x virus treatment. To recollect volatile emissions for analysis, we eluted compounds from adsorbent traps using 150 μL of dichloromethane containing two internal standards: n-octane (2 ng/ μL) and nonyl acetate (4 ng/ μL). We stored volatiles at $-80\text{ }^{\circ}\text{C}$ until analysis using gas chromatography and mass spectrometry (Minitab v.17).

We performed volatile separation and analysis using a gas chromatograph (Agilent 7890B) coupled to a flame-ionization detector (FID) and mass spectrometer (5977A) and equipped with a 30 m \times 250 μm \times 0.25 μm Agilent HP-5MS Ultra Inert column. The injector temperature was $250\text{ }^{\circ}\text{C}$, operated in splitless mode, and helium was used as a carrier gas (constant flow rate of 0.9 mL/min). One microliter of sample eluate was injected, after which the GC oven temperature was held at $35\text{ }^{\circ}\text{C}$ for 0.5 min then increased to $240\text{ }^{\circ}\text{C}$ at a rate of $8\text{ }^{\circ}\text{C}/\text{min}$. Post-run, the oven was heated to $275\text{ }^{\circ}\text{C}$ for two minutes before returning to $35\text{ }^{\circ}\text{C}$ for the next run. A post-column splitter attached to the MS and FID allowed simultaneous collection of data for tentative identification (MS) and quantification (FID). The resulting data were analyzed using the software Mass Hunter and Chemstation (Agilent Technologies, Santa Clara, CA US). Volatiles were identified using authentic standards

when available (indicated in figures), or tentatively identified by comparison with the NIST standard reference database (National Institute of Standards and Technology, Gaithersburg, MD, USA). We converted peak areas (FID trace) to the total quantity of volatile compound sampled (in nanograms) based on the area of the internal standard in each chromatogram and divided the quantity of each compound by the total weight of plant enclosed in the sampling dome to correct for differences in plant size. Blends were compared to determine qualitative differences (number of shared/distinct compounds). Total volatile emissions (sum of all compounds) were rank transformed to improve normality and analyzed using a general linear model with bacterial treatment (2 levels) and virus treatment (2 levels) as fixed effects, plus their interaction (Minitab v.17).

Metabolite profiling: phytohormones and primary metabolites

We explored changes in phytohormone production at a key time point in the *M. truncatula* defense response to pea aphids (24 h). This time point was chosen because prior research on Jemalong A17 and the related Jester cultivar demonstrated that resistance against *A. pisum* and *A. kondii* manifests as increases in both jasmonic acid and salicylic acid at 24 h post aphid attack (Gao et al. 2008; Stewart et al. 2016). This is also the time point in which we observed detectable effects of AMV and bacteria on aphid dispersal, which suggests the presence of a recently activated defense response. We performed a factorial experiment with 7–8 plants (6 weeks old) per bacteria x virus x damage treatment. We enclosed one fully expanded branch of each plant in a fine mesh cage with drawstring closures at the top and bottom. Half of the plants in each bacteria x virus treatment received 15 adult aphids (approximating the density of aphids remaining on release plants in choice tests), while the other half remained with just the empty bag as a control. The plants were maintained in a climate-controlled growth chamber under conditions described above for 24 h before tissue was harvested. For phytohormone measurements, we excised the most recently expanded leaf from the apex of the branch (a preferred feeding location), quickly weighed the tissue, enclosed in a 2 mL Eppendorf tube with two stainless steel grinding beads, and flash froze in liquid nitrogen. Medicago plants at the 6–7-week stage produce multiple branches, each quite similar in architecture. Therefore, we chose a paired undamaged, uncaged branch from the same plant to sample for primary metabolite profiling. We excised the most recently expanded leaf in the same manner as described for phytohormone samples. Both samples were then stored at $-80\text{ }^{\circ}\text{C}$. Prior to processing, samples in tubes were ground to a fine powder under liquid nitrogen using a Genogrinder (SPEX Sample Prep).

Free amino acids and simple sugars (glucose, fructose and sucrose) were analyzed in each sample using the methods of (Lisec et al. 2006) and chemicals from Sigma-Aldrich (HPLC or derivatization grade, or higher). Prior to processing, samples were spiked with 60 μ L of an internal standard (Adonitol 0.2 mg/mL) as described (Lisec et al. 2006). 1.4 mL of cold methanol was added and samples were incubated while shaking at 70 °C for 10 min. Each sample then received 750 μ L of chloroform and 1400 μ L of water, followed by vortexing and separation by centrifugation. The supernatant containing extracted polar compounds was removed as two 150 μ L aliquots to Eppendorf tubes. One aliquot was dried under vacuum without heating and the other stored. The dried sample was derivatized with 40 μ L of methoxyamine hydrochloride (20 mg/mL in pyridine) for 120 min at 37 °C while shaking, followed by derivatization with 70 μ L of MSTFA at 37 °C for 30 min. Blanks without leaf tissue, but with internal standards added to blank tubes, were also taken through the procedure. Derivatized compounds in pyridine were analyzed directly using the same instrumentation as for volatile analysis with the exception of the splitter (only mass spectrometer used for detection). Injection volume was 1 μ L with an inlet temperature of 230 °C in splitless mode and a constant helium carrier gas flow set to 1 mL/min. The temperature program began with an isothermal run at 70 °C for 5 min, followed by a ramp of 5 °C/min up to 325 °C and a final heating at 315 °C for 5 min. The instrument was then cooled to 70 °C and equilibrated prior to analysis of the next sample. The transfer line to the mass spectrometer was set to 250 °C and the mass spectrometer source was operated at 200 °C in electron ionization mode (tuned to the manufacturer's specifications). Scanning was set to 2 scans per second with a range of m/z 50–600. The solvent delay was 13 min. Syringe washes were performed using acetone and hexanes. Chemstation software was used for peak deconvolution and integration. We confirmed peak identities for amino acids (protein coding) and sugars (glucose, fructose and sucrose) using authentic reference standards. Peak areas for leaf samples were converted to nanograms using peak areas and the known amount of internal standard added to each sample, then corrected for the weight of leaf tissue collected. If derivatization produced more than one peak for a compound (verified by standards), the amounts for the two products were summed. Statistical analysis of primary metabolites (individual compounds, total amino acids, and total sugars) was performed using weight-corrected values and general linear models with virus treatment, bacterial treatment, and damage treatment as fixed effects (Minitab v.17).

To extract and quantify jasmonic acid and salicylic acid, we followed procedures described in (Schmelz et al. 2004). Briefly, 10 μ L of an internal standard containing 10 mg/ μ L each of dihydro-jasmonic acid (dH-JA) (TCI America,

through VWR, #D3225) and 2-hydroxy-benzoic acid (d5-SA) (ICON, #9059) was added to each sample tube, followed immediately by addition of an extraction solution consisting of propanol and water with HCl. Samples were mixed by vortexing and 1 mL of dichloromethane was added, followed by vortexing for an additional 10 s. Samples were centrifuged, and the organic layers were transferred to 4 mL glass vials and dried. The residue was mixed with 100 μ L of 1:9 methanol: diethyl ether and 2 μ L of 2.0 M trimethylsilyldiazomethane in hexanes. Vials were incubated in the dark for 25 min, then the reaction was quenched by adding 2 μ L of 2.0 M glacial acetic acid in hexanes. The solution was briefly dried to remove solvents and derivatized compounds were recollected onto adsorbent filters (40 mg Hayesep-Q) by incubating vials at 200 °C for 2 min with a gentle vacuum pulling volatilized phytohormones from the headspace through the filter. We eluted compounds into vials by washing filters with 150 μ L of dichloromethane and quantified salicylic acid and the *cis* isomer of jasmonic acid using gas chromatography and mass spectrometry (instruments as described and settings outlined in (Schmelz et al. 2004). The amount of SA and *cis*-JA was calculated relative to respective internal standards (dH-JA and d5-SA) then corrected for the weight of tissue used in each sample. Data were log transformed to improve normality and analyzed using a general linear model with bacterial treatment, virus infection status, and damage treatment as fixed effects and all possible interaction terms included. Post-hoc Tukey tests were performed among treatments for significant main effects (Minitab v.17).

Results

Odor-based aphid preferences and volatile emissions

In Y-tube assays, aphids did not exhibit a preference for AMV-infected plants over healthy plants regardless of the presence of co-colonizing *Sinorhizobium* (Fig. 1). Total volatile emissions were not significantly different among treatments (Bacterial treatment \times Virus treatment, $F = 4.17$, $p = 0.055$) but emissions from non-infected Sino + plants tended to be higher than all other treatments. Although we did not detect statistically significant quantitative differences in overall emissions, there were several qualitative differences among blends. Plants without virus infection released 10 (control, non-infected) and 12 (Sino +, non-infected) compounds respectively, with overlap between blends of 10 shared compounds. Sino + plants tended to release slightly larger quantities of shared compounds relative to controls. In contrast, AMV + plants released only five compounds in detectable

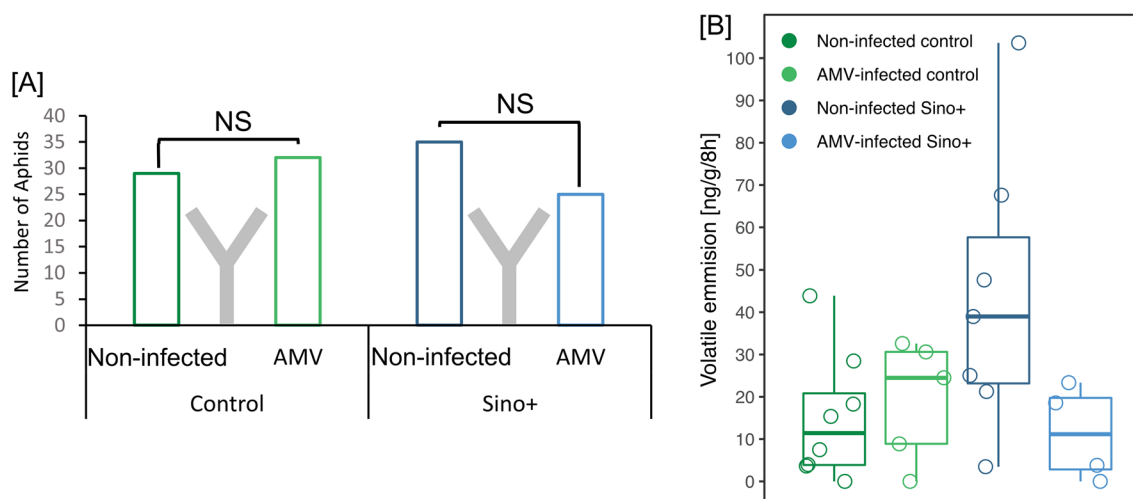


Fig. 1 Odor-based preferences of aphids in dual choice tests (A) and total volatile emissions from plants having different bacteria x virus treatments (B). Aphids did not exhibit a significant preference for AMV-infected plants over non-infected plants regardless of the bac-

terial treatment (Control plants, Chi-squared value=0.148, $df=1$, $p>0.05$; Sino+ plants, Chi-squared value=1.667, $df=1$, $p>0.05$). There were no significant main or interaction terms in the GLM for total volatile emissions among bacteria x virus treatments

amounts regardless of bacterial treatment status, with overlap of four out of five compounds between control and Sino+ treatments (Fig. 2). Overall, these results suggest that AMV infection causes significant qualitative changes in *M. truncatula* volatile blends regardless of whether the plant is associated with *S. meliloti* or not, but that aphids are not responsive to these differences.

Contact-based aphid preferences and transmission assay

In contact-based choice tests, significantly fewer aphids remained on release plants with both AMV and *Sinorhizobium* relative to non-infected plants with *Sinorhizobium*, but AMV infection had no effect on aphid dispersal at two hours in *Sinorhizobium*-free controls (Fig. 3). At 24 h post-release, release plants with both AMV and *Sinorhizobium*

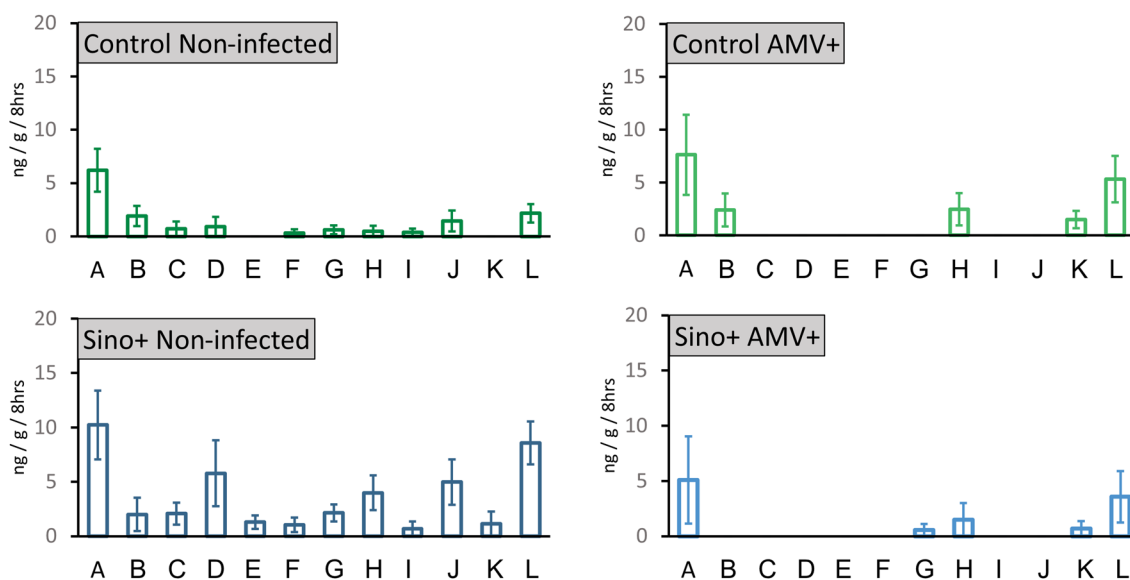


Fig. 2 Volatile compounds emitted by plants under different bacteria x virus treatments. In all graphs, A=Z-3-hexen-1-ol*, B=Z-3-hexen-1-ol acetate*, C=beta ocimene*, D=(E)-4,8-Dimethylnona-1,3,7-triene*, E=Cyclosatirene, F=Copaene, G=Caryophyllene*,

H=Humulene*, I=Germacrene D, J=(E,E)-4,8,12-trimethyl-1,3,7,11-tridecatetraene, K & L unidentified suspected terpenes. * next to the compound names in the prior sentence indicates volatile identities that were confirmed with commercial standards

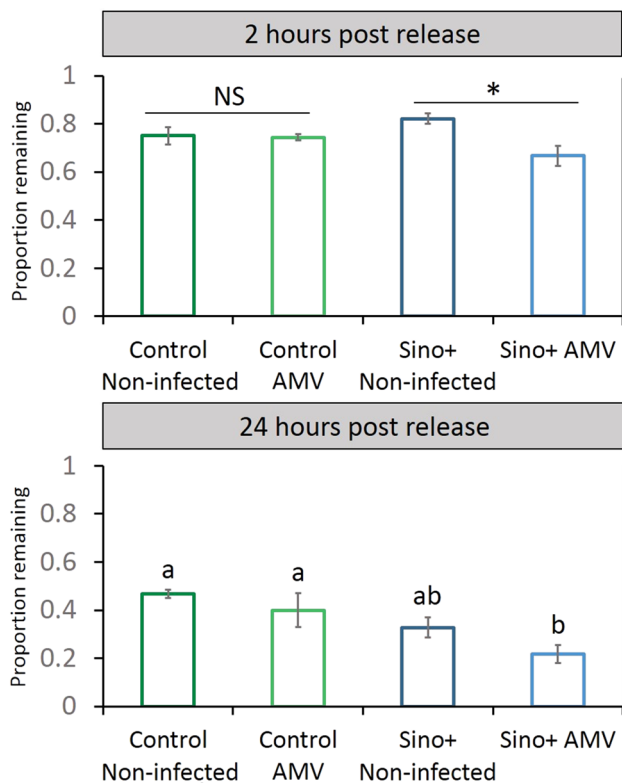


Fig. 3 Aphid dispersal from plants of different bacteria x virus treatments. Data were analyzed as the proportion dispersing from the release plant at each time point. Proportions were log-transformed prior to analysis to meet assumptions of normality. For the 2-h time point, the virus term and bacteria x virus interaction term were statistically significant in the main model (virus $F=6.34$, $p=0.023$; bacteria x virus term $F=5.83$, $p=0.028$). For the 24-h time point, the bacteria and virus terms were statistically significant in the main model (bacteria $F=12.25$, $p=0.003$; virus term $F=5.46$, $p=0.033$). Different letters in each graph indicate significant differences within each analysis following post-hoc Tukey tests ($p < 0.05$)

had retained fewer aphids than both non-infected and AMV-infected controls but were not significantly different from non-infected *Sinorhizobium*-colonized plants (Fig. 3). In transmission tests, significantly more of the susceptible seedlings became infected when the source plant was dual colonized (12.5%) relative to seedlings exposed to source plants that had only AMV but no *S. meliloti* (2.5%) (Fig. 4).

Bacteria and virus effects on phytohormones, metabolites, and plant growth parameters

Neither virus infection status nor bacterial colonization influenced quantities of *cis*-JA or SA in undamaged plants (Fig. 5). Aphid damage did not significantly influence levels of *cis*-JA at the 24 h post-damage time point regardless of bacterial or virus treatment (Fig. 5). Aphid damage did induce production of SA, and this increase was similar across virus treatments when plants were not colonized by

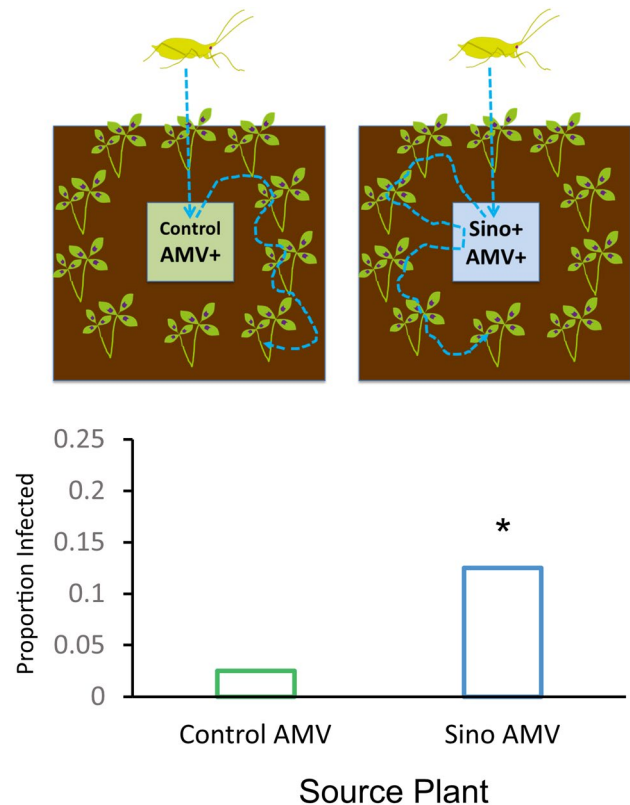


Fig. 4 AMV transmission to susceptible receiver plants from i. The top image is a schematic of the transmission tests with source plants differing in *Sinorhizobium* colonization status. 2.5% of susceptible receiver plants became infected when the AMV source plant was not colonized with *S. meliloti*, while 12.5% of plants became infected when the AMV source plant was co-colonized by *S. meliloti*. This is a significant increase in the proportion of infected plants (two proportion z-test, $z=-1.6979$, $p=0.044$). source plants without and with *S. meliloti*

S. meliloti (Fig. 5). However, when plants were colonized by *S. meliloti* (Sino+), SA was only induced in plants infected with AMV, while non-infected plants had higher baseline levels and showed no evidence of SA induction upon aphid feeding (Fig. 5).

Primary metabolites recovered included 15 proteinogenic amino acids (Table 1) as well as fructose, glucose, and sucrose sugars (Fig. 6). AMV infection was the primary driver of differences in free amino acid content of leaves, with a significant “virus” term in the model for 11/15 amino acids and for the total amino acid quantity (Table 1). In all cases, virus infection lowered amino acid quantities in leaf tissue. Bacterial treatment influenced quantities of tyrosine (higher for Sino+), and there was a significant bacteria x virus treatment interaction for glycine; AMV-infected Sino+ plants had lower quantities of glycine than AMV+ and non-infected control plants (Table 1). *Sinorhizobium* colonization had few effects on amino acid composition (only glycine levels in virus-free Sino+ plants were

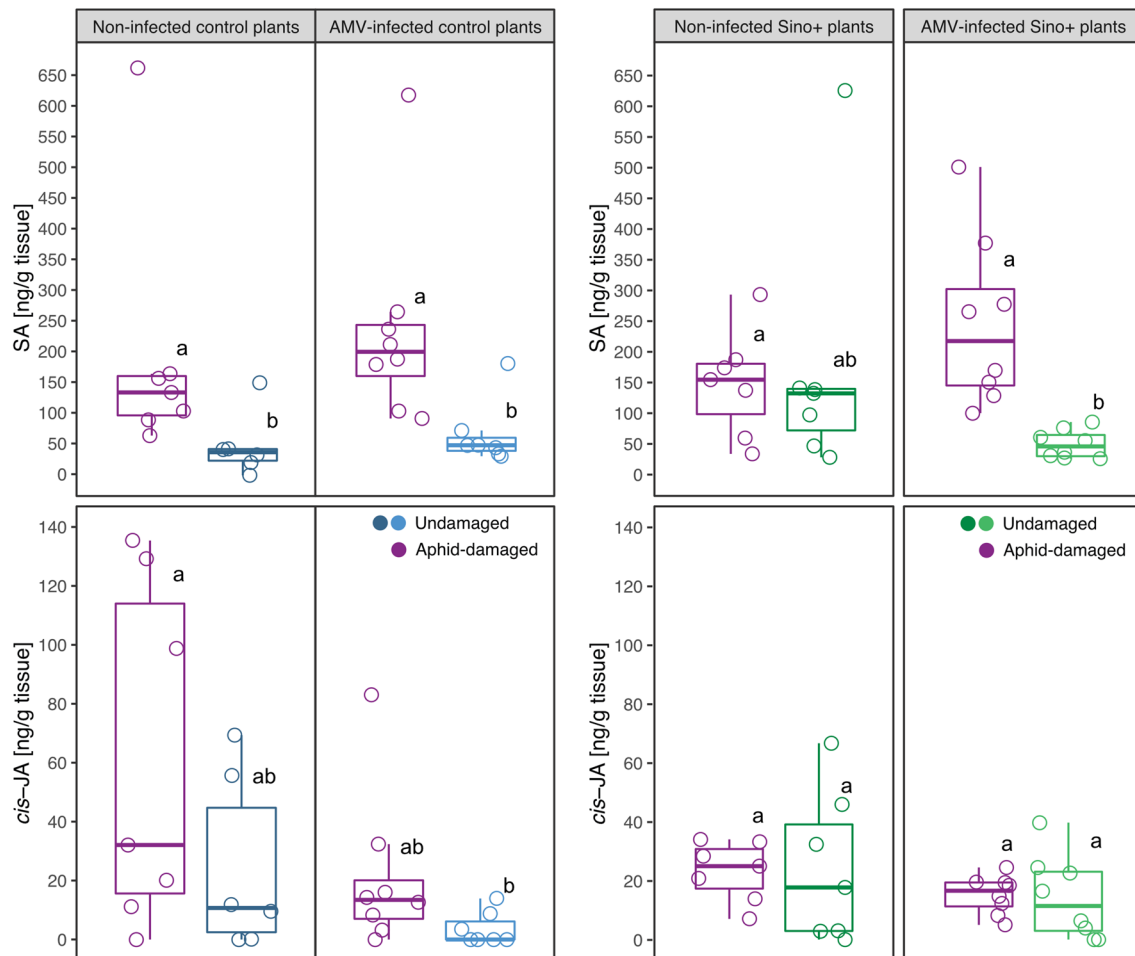


Fig. 5 Phytohormone levels by bacteria x virus treatment, with and without aphid damage. Dots represent individual data points. The lower and upper edges of boxes represent the first and third quartiles, with the horizontal line inside representing the median value. Whiskers extend to the highest and lowest data points within $1.5 \times$ the interquartile range. Graphs at left show data for SA and *cis*-JA in control plants under different virus x damage treatments. The GLM for SA had a significant damage term ($F=29.61$, $p=0.000$) with all other terms non-significant. Data for SA were rank transformed before analysis to meet assumptions of normality. The GLM for *cis*-JA had a significant damage term ($F=5.27$, $p=0.031$) with all other terms

(virus, and virus x damage) non-significant. Data for *cis*-JA were log transformed before analysis to meet assumptions of normality. Graphs at right show data for SA and *cis*-JA for *Sinorhizobium* colonized plants under different virus x damage treatments. The GLM for SA had a significant damage term ($F=13.68$, $p=0.001$) and a significant virus x damage interaction term ($F=6.53$, $p=0.017$). The GLM for *cis*-JA had no significant main or interaction terms. Data for *cis*-JA were log transformed before analysis to meet assumptions of normality. Letters indicate significant differences among treatments within each graph as determined by post-hoc Tukey tests ($p < 0.05$), with $n=7-8$ plants per bacteria x virus x damage treatment

significantly higher than those in virus-free control plants), which indicates that our high-nitrogen vs. low-nitrogen fertilizer treatments successfully produced plants that differed in bacterial association without dramatic differences in nutrient content. AMV infection reduced leaf fructose levels in the presence of *S. meliloti*, but not in control plants, although virus infection overall reduced fructose levels (Fig. 6). Glucose levels were reduced by microbial colonization regardless of which microbe was associated with the plant (bacteria or virus) (Fig. 6). Sucrose levels were not affected by *S. meliloti* colonization or AMV infection. Total sugar quantities (sum of fructose, glucose, and sucrose) were

significantly reduced by AMV infection in Sino+ plants but were not significantly reduced by AMV infection in control plants (Fig. 6).

Plant growth parameters were influenced by both virus infection and *S. meliloti* colonization, but effects depended on plant part (shoot vs. root) (Fig. 7). Virus infection reduced shoot/stem weight regardless of the bacterial treatment, while *S. meliloti* reduced root weight, but AMV infection did not (Fig. 7). The effects of *S. meliloti* on roots resulted in a significantly higher stem:root ratio for Sino+ plants, which was apparent regardless of virus infection status. For reciprocal interactions, virus titer was slightly elevated in

Table 1 Quantities of amino acids in leaf tissue (ng/g fresh weight) and significance of model terms

Amino Acid	Control		Sino+		Significant terms in model
	Non-infected	AMV	Non-infected	AMV	
Leucine	1.058 ± 0.118	0.712 ± 0.073	0.761 ± 0.088	0.871 ± 0.155	None
Isoleucine	0.0 ± 0.0	0.012 ± 0.008	0.006 ± 0.003	0.003 ± 0.001	None
Valine	2.327 ± 0.528	1.998 ± 0.281	2.470 ± 0.430	1.119 ± 0.274	Virus (F=5.08, P=0.028)
Serine	44.502 ± 3.950	30.984 ± 4.325	43.094 ± 4.490	19.964 ± 3.164	Virus (F=20.45, P=0.000)
Threonine	22.492 ± 1.731	18.2 ± 1.579	23.71 ± 1.657	14.344 ± 1.821	Virus (F=15.49, P=0.000)
Glycine	4.567 ± 0.527(ab)	3.325 ± 0.455(bc)	5.968 ± 0.550(a)	2.550 ± 0.518(c)	Virus (F=20.00, P=0.000) Bacteria x Virus (F=4.36, P=0.042)
Methionine	4.820 ± 0.991	2.3 ± 0.538	4.343 ± 0.473	1.910 ± 0.424	Virus (F=17.33, P=0.000)
Aspartic Acid	303.346 ± 29.874	287.09 ± 18.233	337.0 ± 17.318	257.584 ± 22.178	Virus (F=7.62, P=0.008)
Phenylalanine	4.372 ± 0.483	3.206 ± 0.245	4.114 ± 0.527	2.993 ± 0.373	Virus (F=7.62, P=0.008)
Cysteine	0.015 ± 0.007	0.005 ± 0.003	0.039 ± 0.011	0.008 ± 0.004	Virus (F=9.63, P=0.003)
Proline	0.967 ± 0.098	1.191 ± 0.135	1.257 ± 0.202	0.995 ± 0.101	None
Glutamic acid	392.695 ± 27.693	362.502 ± 27.693	412.808 ± 27.693	325.994 ± 27.693	Virus (F=6.69, P=0.013)
Tyrosine	2.446 ± 0.214	1.567 ± 0.233	2.959 ± 0.279	2.225 ± 0.334	Bacteria (F=4.26, P=0.044) Virus (F=8.07, P=0.006)
Lysine	0.655 ± 0.151	0.324 ± 0.044	0.594 ± 0.076	0.414 ± 0.040	Virus (F=10.80, P=0.002)
Tryptophan	0.004 ± 0.002	0.006 ± 0.002	0.005 ± 0.002	0.007 ± 0.003	None
Total	785.175 ± 58.314	714.341 ± 41.857	840.133 ± 41.968	632.084 ± 46.630	Virus (F=8.76, P=0.005)

$n = 14$ – 16 samples per bacteria x virus treatment

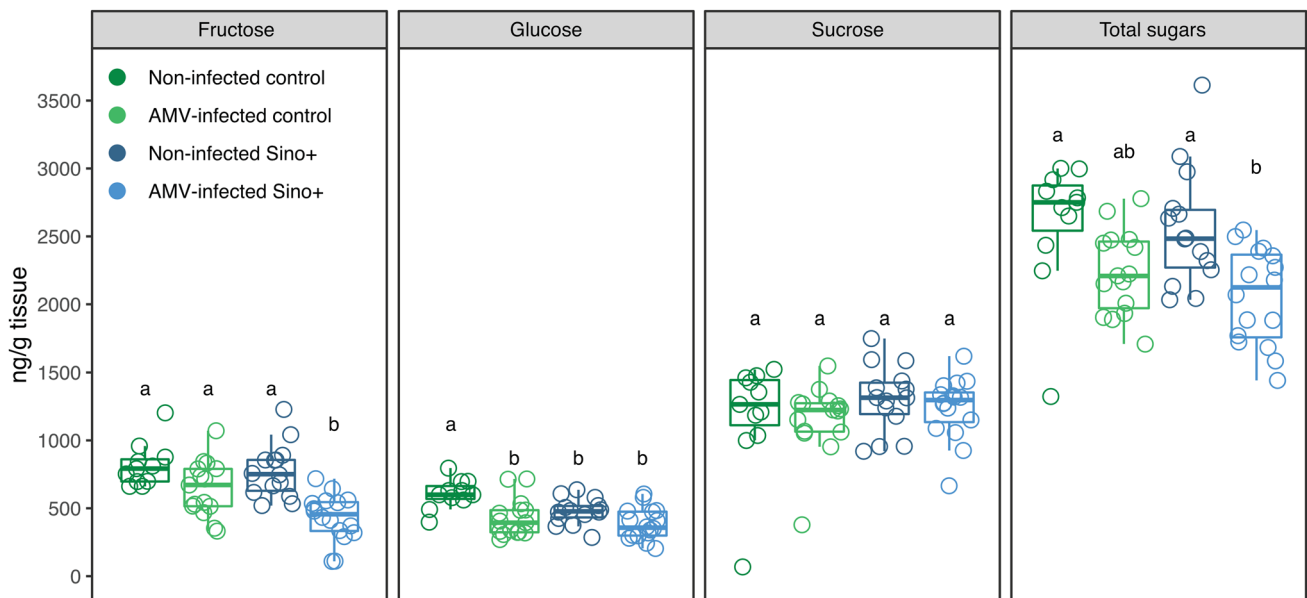


Fig. 6 Quantities of simple sugars in leaf tissue of plants with different bacteria and virus treatments. Dots represent individual data points. The lower and upper edges of boxes represent the first and third quartiles, with the horizontal line inside representing the median value. Whiskers extend to the highest and lowest data points within $1.5 \times$ the interquartile range. The general linear model (GLM) for fructose had significant bacteria ($F=6.43$, $p=0.014$) and virus terms ($F=25.79$, $p=0.000$). The GLM for glucose also had significant bac-

teria ($F=7.59$, $p=0.008$) and virus terms ($F=18.67$, $p=0.000$). The GLM for sucrose did not have any significant main terms or interaction terms. For total sugars, only the virus term was significant ($F=16.95$, $p=0.000$). Data for total sugars were log transformed before analysis to meet assumptions of normality. For all compounds, letters indicate significant differences among bacteria x virus treatment ($n = 14$ – 16 / bacteria x virus treatment)

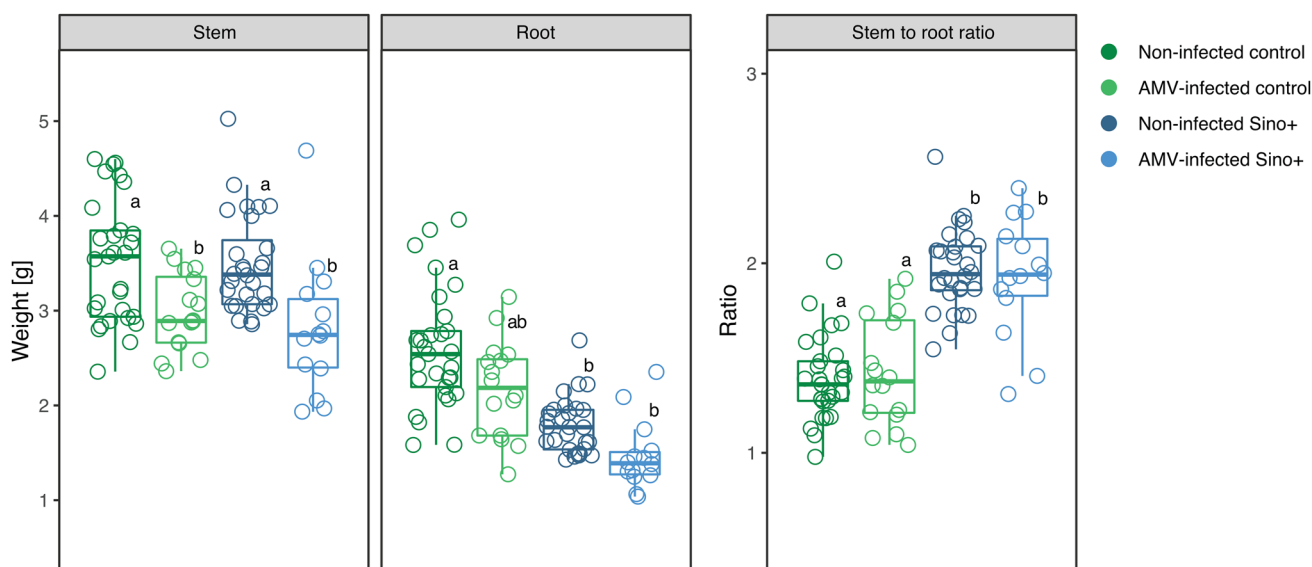


Fig. 7 Plant shoot and root growth by bacteria and virus treatments. Dots represent individual data points. The lower and upper edges of boxes represent the first and third quartiles, with the horizontal line inside representing the median value. Whiskers extend to the highest and lowest data points within $1.5 \times$ the interquartile range. Significant terms in the GLM for stem were set ($F=4.72$, $p=0.011$) and virus infection ($F=25.75$, $p=0.000$). Significant terms in the GLM for root were bacteria ($F=47.51$, $p=0.000$) and virus infec-

tion ($F=11.69$, $p=0.001$). In the GLM for stem:root ratio, bacteria ($F=93.46$, $p=0.000$) was the only significant term. For all graphs, letters indicate significant differences among bacteria \times virus treatment as determined by post-hoc Tukey tests ($p < 0.05$). Due to infection rates below 100%, $n=14$ – 16 plants in control AMV+ and Sino+AMV+ treatments and 28–29 plants in control non-infected and Sino+ non-infected treatments

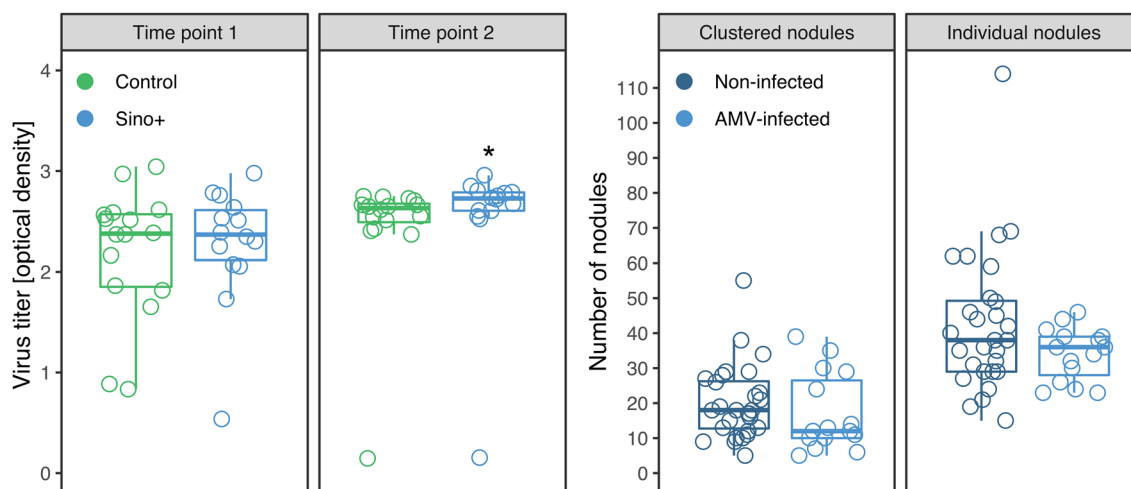


Fig. 8 Effects of *S. meliloti* colonization on virus titer (left) and virus infection on *S. meliloti* nodulation (right). Dots represent individual data points. The lower and upper edges of boxes represent the first and third quartiles, with the horizontal line inside representing the median value. Whiskers extend to the highest and lowest data points within $1.5 \times$ the interquartile range. Titer is expressed as the optical density of tissue quantity standardized ELISA assays and was measured at 28 days after planting (14 days post-inoculation) and at 48 days post-planting (34 days post inoculation). Virus titer was

significantly higher in Sino+ plants at the 48-day time point. For nodulation intensity, nodules were categorized into two morphological types: clustered (consisting of 2+ nodules fused together) and individual (consisting of a single, discrete nodule). Virus infection did not significantly influence either nodule type. For all data, due to infection rates below 100%, $n=14$ – 16 plants in control AMV+ and Sino+AMV+ treatments and 28–29 plants in control non-infected and Sino+ non-infected treatments

the presence of *S. meliloti*, but bacterial nodulation was not significantly altered by virus infection (Fig. 8).

Discussion

Using a co-evolved rhizobia-host-virus system and wild microbe isolates, we explored whether plant virus effects on host phenotype and vector behavior depend on the presence of rhizobia that commonly associate with *Medicago* hosts in the natural environment. We found evidence that rhizobia-colonized hosts infected with AMV were the least preferred based on contact cues, but the most effective as sources of inoculum in semi-natural vector dispersal events, producing five times more new infections than AMV-infected hosts without rhizobia colonization. This finding supports our original hypothesis that the presence of *S. meliloti* as a co-colonizer of the host plant would modify virus effects on plant phenotype and vector behavior. Subsequent experiments exploring defense induction and nutrient composition of hosts with different bacteria x virus treatments do not provide a clear mechanism underlying this phenotype but suggest that reduced aphid preferences for plants having both *Sinorhizobium* colonization and AMV infection may be mediated by maintenance of anti-aphid defenses (SA induction) in combination with reduced levels of amino acids and some phagostimulatory sugars. Overall, our results suggest that AMV is more successful in manipulating the host and vector in the presence of *S. meliloti*.

Our study provides evidence that plant virus effects on host phenotypes, and especially putative manipulations of vector behavior, can be influenced by the pre-existing physiological condition of the host—in this case, presence of a co-evolved intracellular root symbiont. This work adds to a small, but growing number of studies that document context-dependency of putative “manipulations” of host phenotype and vector behavior. For example, Ángeles-López et al. (2018) found that effects of *Pepper golden mosaic virus* on host plants that attract and arrest a particular whitefly vector species were counteracted when a non-vector whitefly feeds on the plant. More recently, we found that manipulation of whitefly attraction to infected hosts by *Cucurbit yellow stunting disorder virus* is only evident at later stages of disease progression (Chesnais et al. 2021) and that pre-activation of SA-regulated defense pathways disrupts this manipulative phenotype (Kenney et al. 2020). In the present study, putative manipulation of host phenotype and vector behavior was evident for AMV when the co-evolved bacterial symbiont was present. When plants were not associated with their symbiont (but had equivalent nutrients), there was no evidence of manipulative effects; AMV infection did not alter attractiveness or palatability of control plants lacking *Sinorhizobium* relative to non-infected controls.

Transmission assays that link behavioral observations to outcomes for virus fitness also suggest that infections in *Sinorhizobium*-associated plants are more beneficial for this particular isolate of AMV.

Our data on reciprocal interactions among AMV and *Sinorhizobium* within the shared host provide further support for our conclusion that infections in rhizobia-colonized plants can improve virus fitness. In contrast to a previous study on *Medicago* (Wahyuni and Randles 1993), we found that for this particular combination of microbe, host, and virus, *Sinorhizobium* colonization did not increase host resistance to AMV, with virus titers equal to or greater than those in rhizobia-free hosts. *Sinorhizobium* colonization also shifted resource allocation in the host to favor shoot over root tissue; colonized plants produced equivalent shoot tissue as controls with less allocation to roots. This is in line with natural variation in rhizobia effects on host resource partitioning and root biomass, with some rhizobia genotypes enhancing and others reducing root production (Laguerre et al. 2007). Additionally, while we did detect overall reductions in root biomass due to virus infection, which has been documented in other studies (Malmstrom et al. 2017), we did not detect negative effects of AMV on nodule numbers: nodule quantities on roots of infected plants were similar to those on roots of rhizobia-free plants. This contrasts with prior studies documenting reductions in nodulation in *Medicago* (Wroth et al. 1993) and soybean (Pulido et al. 2019) during virus infections.

When considering these effects, it is important to note that the microbes used in our study were isolated locally from closely congeneric hosts of *M. truncatula* (*Medicago lupulina* for the *Sinorhizobium* spp. and unmanaged *Medicago sativa* for AMV) and used for experiments with as little in-lab propagation as possible (only that required to obtain pure cultures). This intentional aspect of our methodology stands in sharp contrast to nearly all other studies documenting putative instances of virus manipulation, the overwhelming majority of which focus on infections by viruses that have been in laboratory culture for years or even decades, with largely unknown host-passage histories (Mauck et al. 2018). Such methods are likely to impose selection regimes on virus populations that do not represent those encountered in the field (e.g. selecting for highly symptomatic hosts), and are independent of vector preferences. Putative manipulative effects documented for viruses maintained in this way should therefore be considered preliminary until confirmed in natural or semi-natural environments (Mauck 2016; Mauck et al. 2018). In the present study, we were not able to include genetically distinct field and laboratory cultured rhizobia and AMV to rigorously test hypotheses about how field vs. laboratory propagation influences virus-induced host phenotypes. However, our observation of benign to beneficial interactions between AMV and

Sinorhizobium recently isolated from *Medicago* hosts, in the context of putative manipulations by AMV, suggests that future work on both virus manipulation and virus pathology in hosts should consider microbial provenance.

Using chemical analyses of plant volatiles, phytohormones (*cis*-JA and SA), and nutrients (sugars and amino acids), we attempted to parse the mechanisms underlying vector behavioral responses to plants with different bacteria x virus treatments. Phytohormone induction shows specificity based on molecular patterns associated with the attacker and determines the intensity of downstream anti-herbivore and anti-pathogen responses (Schmelz et al. 2009; Erb et al. 2012). Defense induction following pea aphid feeding has previously been studied for the particular genotype of *M. truncatula* employed here (Gao et al. 2008), with results demonstrating that JA-regulated defenses are not strongly induced by aphid feeding, while SA-regulated defenses are active against pea aphids between 24 and 36 h after the start of feeding damage. Consistent with this, we did not detect significant induction of *cis*-JA at 24 h post aphid feeding regardless of bacteria x virus treatment but did detect significant induction of SA in all treatments lacking *Sinorhizobium* colonization, regardless of AMV infection status. Non-infected *Sinorhizobium* plants did not produce greater SA following aphid feeding. However, when *Sinorhizobium*-colonized plants were infected with AMV, this restored inducibility of SA in response to aphid attack. Since SA mediates aphid resistance in *M. truncatula* (Gao et al. 2008) this result indicates that AMV infection may counteract *Sinorhizobium* suppression of the anti-aphid response. Evidence for this comes from a study of AMV infection in the model plant, *Arabidopsis thaliana*, where the AMV coat protein functioned as an SA elicitor by interacting with a transcription factor (ILR3) and causing re-localization from the nucleus to the nucleolus (Aparicio and Pallás 2017). The effect of this AMV-driven re-localization partially mimics the phenotype that occurs in mutants lacking ILR3 function; SA accumulation and activation of multiple plant defense pathways (Aparicio and Pallás 2017).

In addition to responding to aphid attack with SA induction, AMV-infected *Sinorhizobium*-colonized plants had the lowest average quantities of nutrients overall and significantly lower quantities of some compounds that are important for pea aphid preferences. For example, fructose was significantly reduced in *Sinorhizobium*-colonized leaf tissue infected with AMV relative to all other treatments. Fructose is a phagostimulant for some aphid species (Hewer et al. 2010), and pea aphids have very high rates of fructose assimilation across the gut wall, with fructose being the primary sugar used as a substrate for respiration (Ashford et al. 2000). As leaf tissue (mesophyll cell) contents are sampled by aphids during initial assessments of plants and during stylet navigation to phloem elements (Martin et al. 1997;

Hewer et al. 2011), lower quantities of fructose in leaf tissue may partly explain the reduced aphid preference for dual-colonized plants observed at two hours post contact in our behavioral assays.

AMV-infected plants also had significantly reduced levels of free amino acids in leaf tissue, with AMV-infected *Sinorhizobium*-colonized plants specifically having significantly lower levels of glycine than non-infected *Sinorhizobium*-colonized plants (which had slightly elevated levels). The mechanisms behind virus-induced changes in amino acid pools are not known for AMV, but such alterations are frequently reported for virus-infected plants (Mauck et al. 2018). Functional genomics studies show that changes in multiple amino acids can even be mediated by the effects of single viral proteins, such as the nuclear inclusion a-protease domain (NIa-Pro) protein encoded by *Turnip mosaic virus* (*Potyvirus*, family *Potyviridae*) (Casteel et al. 2014). Overall, the less palatable phenotype of *Sinorhizobium*-colonized, AMV-infected plants may be a product of constitutive differences in both sugar and amino acid concentrations in combination with inducible anti-aphid defenses. Future experiments could explore this hypothesis by quantifying defense gene expression and changes in metabolites over a time course of aphid feeding (Gao et al. 2008), and at different points in disease progression (Chesnais et al. 2021).

While we did find evidence that AMV effects on host palatability and quality for aphids depend partly on co-occurring rhizobia, we did not find evidence that AMV alters vector behavior via effects on host volatile emissions. Many studies across diverse pathosystems have now documented preferential attraction of vectors to the volatile emissions of infected hosts over non-infected hosts (reviewed in Mauck et al. 2016, 2018). In our study, volatile profiles were strongly affected by AMV infection, which reduced the number of compounds emitted in detectable amounts from 10 to 12 to five. These effects on volatile blend persisted regardless of whether the plant was colonized by *Sinorhizobium*. Aphid preferences tended to track with overall quantity of volatiles emitted, consistent with prior studies documenting increased attraction to sources emitting larger quantities of volatiles (Ngumbi et al. 2007; Mauck et al. 2010, 2014). However, aphids did not discriminate between blends of non-infected and infected hosts in either bacterial treatment, despite markedly reduced complexity in the blends of infected hosts. This could be because the blends of infected plants retain key compounds indicative of host identity in similar quantities and ratios as those of non-infected host blends (e.g., *Z*-3-hexen-1-ol, humulene, and two terpenes that could not be identified). Alternatively, pea aphids may not be strongly responsive to variation in volatile blends emitted from certain hosts. In a prior study documenting responses of three pea aphid genotypes to pea and alfalfa hosts with and without infection by *Bean leafroll*

virus, Davis et al. (2017) found that two genotypes of pea aphids preferred pea over alfalfa (*Medicago sativa*) regardless of infection status in choice tests permitting access to contact and gustatory cues, but no significant preferences when assays only permitted volatile cues. If volatile cues are not primary drivers of pea aphid preference in nature, it is logical to conclude that there could be weak selection pressure on a virus to manipulate this type of cue.

By combining recently isolated microbial associates with a legume host that has undergone minimal artificial selection for agronomic traits, this study addresses important gaps in the study of virus manipulation of host phenotypes and vector behavior. Our findings indicate that a plant virus can experience higher fitness, both within a host (replication) and between hosts (number of new infections), when infecting plants that are in association with a co-evolved, intracellular, rhizobia symbiont. In the absence of this symbiont, we found no evidence of putative virus manipulations of host phenotype and vector behavior. We also found no evidence of antagonistic effects between virus and bacterial symbionts, while the host experienced trade-offs in growth or defense because of each association. Overall, our findings underscore the importance of considering virus effects on host phenotypes in an ecological context that includes other core microbial associates. An increased focus on virus manipulation in ecological contexts will provide greater mechanistic insight into the genetic drivers of manipulative traits in pathogens as well as strategies to counteract virus manipulations in agricultural settings.

Supplementary Information The online version contains supplementary material available at <https://doi.org/10.1007/s11829-021-09878-6>.

Acknowledgements Thanks to James Sims for assistance with GC-MS operation and Monika Maurhofer for advice on bacterial culture techniques. Thanks also to Dinka Matic Velkic and Anna Dalbosco for many great discussions on root bacteria and plant defense.

Authors' contributions KEM designed the study along with CMD and MCM. KEM, MN, and LG planned and executed experiments and performed analyses. All authors contributed to manuscript drafting and revision.

Funding This work was supported by an ETH Zurich Postdoctoral Research Fellowship to KEM (FEL-44 14–1), Hatch project funds to KEM (CA-R-ENT-5144-H), and by startup funds provided to CMD and MCM.

Data availability Upon publication, all data will be deposited in the DRYAD data repository.

Declarations

Conflict of interest The authors declare that they have no conflict of interest. The funders had no role in the design of the study, in the analyses, or interpretation of data; in the writing of the manuscript, or in the decision to publish the results.

Ethical approval No ethical approvals were required to conduct this study.

Consent for publication All authors consent to the publication of this work.

References

- Ángeles-López YI, Rivera-Bustamante R, Heil M (2018) Fatal attraction of non-vector impairs fitness of manipulating plant virus. *J Ecol* 106:391–400
- Aparicio F, Pallás V (2017) The coat protein of *Alfalfa mosaic virus* interacts and interferes with the transcriptional activity of the bHLH transcription factor ILR3 promoting salicylic acid-dependent defence signalling response. *Mol Plant Pathol* 18:173–186. <https://doi.org/10.1111/mpp.12388>
- Ashford DA, Smith WA, Douglas AE (2000) Living on a high sugar diet: the fate of sucrose ingested by a phloem-feeding insect, the pea aphid *Acyrtosiphon pisum*. *J Insect Physiol* 46:335–341. [https://doi.org/10.1016/s0022-1910\(99\)00186-9](https://doi.org/10.1016/s0022-1910(99)00186-9)
- Ballhorn DJ, Kautz S, Schädler M (2013) Induced plant defense via volatile production is dependent on rhizobial symbiosis. *Oecologia* 172:833–846. <https://doi.org/10.1007/s00442-012-2539-x>
- Barbetti MJ, Pei You M, Jones RAC (2020) *Medicago truncatula* and other annual *Medicago* spp. – interactions with root and foliar fungal, oomycete, and viral pathogens. *The Model Legume Medicago truncatula* 293–306
- Blackmer JL, Cañas LA (2005) Visual cues enhance the response of *Lygus hesperus* (Heteroptera: Miridae) to volatiles from host plants. *Environ Entomol* 34:1524–1533. <https://doi.org/10.1603/0046-225X-34.6.1524>
- Cachapa JC, Meyling NV, Burow M, Hauser TP (2021) Induction and priming of plant defense by root-associated insect-pathogenic fungi. *J Chem Ecol* 47:112–122. <https://doi.org/10.1007/s10886-020-01234-x>
- Casteel CL, Yang C, Nanduri AC et al (2014) The NIa-Pro protein of Turnip mosaic virus improves growth and reproduction of the aphid vector, *Myzus persicae* (green peach aphid). *Plant J* 77:653–663. <https://doi.org/10.1111/tpj.12417>
- Chesnais Q, Sun P, Mauck KE (2021) Advanced infections by cucurbit yellow stunting disorder virus encourage whitefly vector colonization while discouraging non-vector aphid competitors. *J Pest Sci*. <https://doi.org/10.1007/s10340-021-01394-z>
- Dall DJ, Randles JW, Francki R (1989) The effect of alfalfa mosaic virus on productivity of annual barrel medic, *Medicago truncatula*. *Aust J Agric Res* 40:807–815. <https://doi.org/10.1071/ar9890807>
- Davis TS, Wu Y, Eigenbrode SD (2017) The effects of bean leafroll virus on life history traits and host selection behavior of specialized pea aphid (*Acyrtosiphon pisum*, Hemiptera: Aphididae) genotypes. *Environ Entomol* 46(1):68–74
- Dean JM, Mescher MC, De Moraes CM (2009) Plant–rhizobia mutualism influences aphid abundance on soybean. *Plant Soil* 323:187–196. <https://doi.org/10.1007/s11104-009-9924-1>
- Dean JM, Mescher MC, De Moraes CM (2014) Plant dependence on rhizobia for nitrogen influences induced plant defenses and herbivore performance. *Int J Mol Sci* 15:1466–1480. <https://doi.org/10.3390/ijms15011466>
- Erb M, Meldau S, Howe GA (2012) Role of phytohormones in insect-specific plant reactions. *Trends Plant Sci* 17:250–259. <https://doi.org/10.1016/j.tplants.2012.01.003>
- Friman J, Pineda A, Loon JJA, Dicke M (2020) Bidirectional plant-mediated interactions between rhizobacteria and shoot-feeding

- herbivorous insects: a community ecology perspective. *Ecol Entomol* 9:1239. <https://doi.org/10.1111/een.12966>
- Gao L-L, Klingle JP, Anderson JP et al (2008) Characterization of pea aphid resistance in *Medicago truncatula*. *Plant Physiol* 146:996–1009. <https://doi.org/10.1104/pp.107.111971>
- Gourion B, Berrabah F, Ratet P, Stacey G (2015) Rhizobium–legume symbioses: the crucial role of plant immunity. *Trends Plant Sci* 20:186–194. <https://doi.org/10.1016/j.tplants.2014.11.008>
- Hewer A, Will T, van Bel AJE (2010) Plant cues for aphid navigation in vascular tissues. *J Exp Biol* 213:4030–4042. <https://doi.org/10.1242/jeb.046326>
- Hewer A, Becker A, van Bel AJE (2011) An aphid's Odyssey—the cortical quest for the vascular bundle. *J Exp Biol* 214:3868–3879
- ICTV (2019) Genus: Alfamovirus. The online (10th) Report of the International Committee on Taxonomy of Viruses. https://talk.ictvonline.org/ictv-reports/ictv_online_report/positive-sense-rnaviruses/w/bromoviridae/1105/genus-alfamovirus.
- Jaspars EM, Bos L (1980) Alfalfa mosaic virus. N°229. In: Description of plant viruses. Kew, England, England: Commonwealth Mycology Institute/Association of Applied Biologists. <https://www.dpvweb.net/dpv/showdpv/?dpvno=229>.
- Jones RAC (2012) Virus diseases of annual pasture legumes: incidences, losses, epidemiology, and management. *Crop Pasture Sci* 63:399–418. <https://doi.org/10.1071/CP12117>
- Kenney JR, Grandmont M-E, Mauck KE (2020) Priming melon defenses with acibenzolar-S-methyl attenuates infections by phylogenetically distinct viruses and diminishes vector preferences for infected hosts. *Viruses* 12:257. <https://doi.org/10.3390/v12030257>
- Laguette G, Depret G, Bourion V, Duc G (2007) Rhizobium leguminosarum bv. viciae genotypes interact with pea plants in developmental responses of nodules, roots and shoots. *New Phytol* 176:680–690. <https://doi.org/10.1111/j.1469-8137.2007.02212.x>
- Lefèvre T, Thomas F (2008) Behind the scene, something else is pulling the strings: Emphasizing parasitic manipulation in vector-borne diseases. *Infect Genet Evol* 8:504–519. <https://doi.org/10.1016/j.meegid.2007.05.008>
- Lisee J, Schauer N, Kopka J et al (2006) Gas chromatography mass spectrometry–based metabolite profiling in plants. *Nat Protoc* 1:387–396. <https://doi.org/10.1038/nprot.2006.59>
- Löser TB, Mescher MC, De Moraes CM, Maurhofer M (2021) Effects of root-colonizing fluorescent *Pseudomonas* on *Arabidopsis* resistance against a pathogen and an herbivore. *Appl Environ Microbiol*. <https://doi.org/10.1128/AEM.02831-20>
- Maclot F, Candresse T, Filloux D et al (2020) Illuminating an ecological blackbox: Using high throughput sequencing to characterize the plant virome across scales. *Front Microbiol* 11:2575. <https://doi.org/10.3389/fmicb.2020.578064>
- Malmstrom CM, Bigelow P, Trębicki P et al (2017) Crop-associated virus reduces the rooting depth of non-crop perennial native grass more than non-crop-associated virus with known viral suppressor of RNA silencing (VSR). *Virus Res* 241:172–184. <https://doi.org/10.1016/j.virusres.2017.07.006>
- Martin B, Collar JL, Tjallingii WF et al (1997) Intracellular ingestion and salivation by aphids may cause the acquisition and inoculation of non-persistently transmitted plant viruses. *J Gen Virol* 78:2701–2705
- Mauck KE (2016) Variation in virus effects on host plant phenotypes and insect vector behavior: what can it teach us about virus evolution? *Curr Opin Virol* 21:114–123. <https://doi.org/10.1016/j.coviro.2016.09.002>
- Mauck KE, Chesnais Q (2020) A synthesis of virus-vector associations reveals important deficiencies in studies on host and vector manipulation by plant viruses. *Virus Res* 285:197957. <https://doi.org/10.1016/j.virusres.2020.197957>
- Mauck KE, De Moraes CM, Mescher MC (2010) Deceptive chemical signals induced by a plant virus attract insect vectors to inferior hosts. *Proc Natl Acad Sci U S A* 107:3600–3605. <https://doi.org/10.1073/pnas.0907191107>
- Mauck KE, De Moraes CM, Mescher MC (2014) Evidence of local adaptation in plant virus effects on host–vector interactions. *Integr Comp Biol* 54:193–209. <https://doi.org/10.1093/icb/ictu012>
- Mauck KE, De Moraes CM, Mescher MC (2016) Effects of pathogens on sensory-mediated interactions between plants and insect vectors. *Curr Opin Plant Biol* 32:53–61. <https://doi.org/10.1016/j.pbi.2016.06.012>
- Mauck KE, Chesnais Q, Shapiro LR (2018) Evolutionary determinants of host and vector manipulation by plant viruses. *Adv Virus Res* 101:189–250. <https://doi.org/10.1016/bs.aivir.2018.02.007>
- Mauck K, Bosque-Pérez NA, Eigenbrode SD (2012) Transmission mechanisms shape pathogen effects on host–vector interactions: evidence from plant viruses. *Functional*
- McLeish M, Sacristán S, Fraile A, García-Arenal F (2019) Coinfection organizes epidemiological networks of viruses and hosts and reveals hubs of transmission. *Phytopathology* 109:1003–1010. <https://doi.org/10.1094/PHYTO-08-18-0293-R>
- Ngumbi E, Eigenbrode SD, Bosque-Pérez NA et al (2007) *Myzus persicae* is arrested more by blends than by individual compounds elevated in headspace of PLRV-infected potato. *J Chem Ecol* 33:1733–1747. <https://doi.org/10.1007/s10886-007-9340-z>
- Olowe OM, Akanmu AO, Asemoloye MD (2020) Exploration of microbial stimulants for induction of systemic resistance in plant disease management. *Ann Appl Biol* 177:282–293. <https://doi.org/10.1111/aab.12631>
- Partida-Martínez LP, Heil M (2011) The microbe-free plant: fact or artifact? *Front Plant Sci*. <https://doi.org/10.3389/fpls.2011.00100>
- Pulido H, Mauck Kerry E, De Moraes CM, Mescher Mark C (2019) Combined effects of mutualistic rhizobacteria counteract virus-induced suppression of indirect plant defences in soya bean. *Proc R Soc B: Biol Sci* 286:20190211. <https://doi.org/10.1098/rspb.2019.0211>
- Roosien BK, Gomulkiewicz R, Ingwell LL et al (2013) Conditional vector preference aids the spread of plant pathogens: results from a model. *Environ Entomol* 42:1299–1308. <https://doi.org/10.1603/EN13062>
- Schmelz EA, Engelberth J, Tumlinson JH et al (2004) The use of vapor phase extraction in metabolic profiling of phytohormones and other metabolites. *Plant J* 39:790–808. <https://doi.org/10.1111/j.1365-3113X.2004.02168.x>
- Schmelz EA, Engelberth J, Alborn HT et al (2009) Phytohormone-based activity mapping of insect herbivore-produced elicitors. *Proc Natl Acad Sci U S A* 106:653–657. <https://doi.org/10.1073/pnas.0811861106>
- Shates TM, Sun P, Malmstrom CM et al (2018) Addressing research needs in the field of plant virus ecology by defining knowledge gaps and developing wild dicot study systems. *Front Microbiol* 9:3305. <https://doi.org/10.3389/fmicb.2018.03305>
- Shaw AK, Peace A, Power AG, Bosque-Pérez NA (2017) Vector population growth and condition-dependent movement drive the spread of plant pathogens. *Ecology* 98:2145–2157. <https://doi.org/10.1002/ecy.1907>
- Shaw AK, Igoe M, Power AG et al (2019) Modeling approach influences dynamics of a vector-borne pathogen system. *Bull Math Biol*. <https://doi.org/10.1007/s11538-019-00595-z>
- Somasegaran P, Hoben HJ (1994) Handbook for Rhizobia: Methods in Legume–Rhizobium Technology. Springer, New York, NY
- Stewart SA, Hodge S, Bennett M et al (2016) Aphid induction of phytohormones in *Medicago truncatula* is dependent upon time post-infestation, aphid density and the genotypes of both plant and insect. *Arthropod Plant Interact* 10:41–53. <https://doi.org/10.1007/s11829-015-9406-8>
- Thamer S, Schädler M, Bonte D, Ballhorn DJ (2011) Dual benefit from a belowground symbiosis: nitrogen fixing rhizobia promote

- growth and defense against a specialist herbivore in a cyanogenic plant. *Plant Soil* 341:209–219. <https://doi.org/10.1007/s11104-010-0635-4>
- Wahyuni WS, Randles JW (1993) Inoculation with root nodulating bacteria reduces the susceptibility of *Medicago truncatula* and *Lupinus angustifolius* to cucumber mosaic virus (CMV) and addition of nitrate partially reverses the effect. *Aust J Agric Res* 44:1917–1929
- Wang RY, Ghabrial SA (2002) Effect of aphid behavior on efficiency of transmission of soybean mosaic virus by the soybean-colonizing aphid, *Aphis glycines*. *Plant Dis* 86:1260–1264. <https://doi.org/10.1094/PDIS.2002.86.11.1260>
- Wroth JM, Dilworth MJ, Jones RAC (1993) Impaired nodule function in *Medicago polymorpha* L. infected with alfalfa mosaic virus. *New Phytol* 124:243–250. <https://doi.org/10.1111/j.1469-8137.1993.tb03813.x>

Publisher's Note Springer Nature remains neutral with regard to jurisdictional claims in published maps and institutional affiliations.